A first characterization of the NIO1 particle beam by means of a diagnostic calorimeter

A. Pimazzoni, M. Cavenago, V. Cervaro, D. Fasolo, G. Serianni, M. Tollin, and P. Veltri

Citation: AIP Conference Proceedings **1869**, 030028 (2017);
View online: https://doi.org/10.1063/1.4995748
View Table of Contents: http://aip.scitation.org/toc/apc/1869/1
Published by the American Institute of Physics

A First Characterization of the NIO1 Particle Beam by Means of a Diagnostic Calorimeter

A. Pimazzoni[1,2,a)], M. Cavenago[2], V.Cervaro[1],
D. Fasolo[1], G. Seriann[1], M. Tollin[1], P. Veltri[1,2]

[1]*Consorzio RFX, Corso Stati Uniti 4, 35127, Padova (Italy)*
[2]*INFN-LNL, Viale dell'Università 2, 35020, Legnaro (Italy) 3Università degli Studi di Padova, Via 8 Febbraio 2, 35122, Padova (Italy)*

[a)]Corresponding author: antonio.pimazzoni@igi.cnr.it

Abstract. Powerful neutral beam injectors (NBI) are required as heating and current drive systems for tokamaks like ITER. The development of negative ion sources and accelerators (40 A; 1 MeV D- beam) in particular, is a crucial point and many issues still require a better understanding. In this framework, the experiment NIO1 (9 beamlets of 15 mA H^- each, 60 kV) operated at Consorzio RFX started operation in 2014[1]. Both its RF negative ion source (up to 2.5 kW) and its beamline are equipped with many diagnostics [2]. For the early tests on the extraction system, oxygen has been used as well as hydrogen due to its higher electronegativity, which allows reaching currents large enough to test the beam diagnostics even without caesium injection. In particular a 1D-CFC (carbon-fibre-carbon composite) tile is used as a calorimeter to determine the beam power deposition by observing the rear surface of the tile with an infra-red camera; the same design is applied as for STRIKE [3], one of the diagnostics of SPIDER (the ITER-like ion source prototype [4]) whose facility is currently under construction at Consorzio RFX. From this diagnostic it is also possible to assess the beam divergence and thus the beam optics. The present contribution describes the characterization of the NIO1 particle beam by means of temperature and current measurements with different source and accelerator parameters.

INTRODUCTION

The radio frequency (RF) ion source NIO1 (2.5 kW) [5,6] has been designed to generate a H- beam up to 60 kV and 135 mA. The main point of interest for this experiment is that it can operate in continuous mode in conditions similar to those foreseen for larger RF ion sources. On the other hand, thanks to its small size, it can be used as a practical benchmark both for validating codes and testing solutions aiming at increasing the overall beam generation efficiency. For such reasons, NIO1 is equipped with many diagnostics [2]. NIO1 started operation in 2014, and the first studies were devoted to the RF source [5] while tests on the extraction system began in 2015. A global description of the main results of the NIO1 experiment is given in [7].

The acceleration system is made of three grids with 9 apertures each: the so-called plasma grid (PG), facing the plasma of the RF source and kept at negative potential, the extraction grid (EG), and the post-acceleration grid (PA), close to ground potential. The reference potentials are -60 kV for the PG, -50 kV for the EG and 0 kV for the PA. The apertures (radius 3.8 mm) are arranged in a 3 x 3 matrix and spaced by 14 mm. The operator controls the voltage U_{ex} applied to the first gap (generally referred to as extraction voltage) and the total voltage applied between the PG and the PA, U_{tot}.

To remove the co-extracted electrons, permanent magnets are installed in the EG, while a filter field is induced close to the PG by the flow of a current I_{filter} within the PG itself to lower the temperature T_e of the electrons close to the extraction region. This filter is expected to be more effective when the integral of the magnetic field along a particle path is larger. For this reason, different paths have been designed for the current and tested [8]. A bias plate is also installed in the plasma source upstream of the PG to limit the co-

Fifth International Symposium on Negative Ions, Beams and Sources (NIBS 2016)
AIP Conf. Proc. 1869, 030028-1–030028-8; doi: 10.1063/1.4995748
Published by AIP Publishing. 978-0-7354-1549-2/$30.00

extracted electrons [9]. In the interaction between the ion beam and the gas in the drift tube, electrons and positive ions are created. To avoid the backstreaming of positive ions towards the source, another grid, the so-called repeller, whose potential can be raised to a few hundred volts, is placed downstream of the PA. A view of the repeller from inside the NIO1 vacuum vessel is provided in Figure 1. To enhance the H^- production, the possibility to inject caesium in the NIO1 ion source has been foreseen for future operations but has not been exploited yet. This sets a first limit to the achievable current, which is unlikely to reach beyond 15 mA in such a configuration. The currents impinging on the three grids are measured separately.

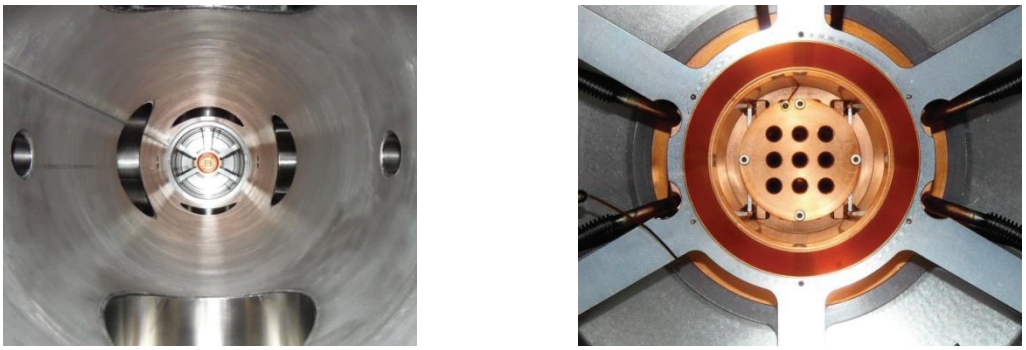

(a) (b)

Figure 1. (a) View of the repeller grid from inside the NIO1 vacuum vessel. (b) Close view of the repeller. The drift tube and water cooling channels are also visible.

The current I_{EG} measured on the EG is composed mostly of co-extracted electrons, as negative ions are much less deflected by the magnetic field due to their higher mass, while the current impinging on the PA can be considered as composed mostly of negative ions and partly of the electrons which are stripped between the EG and the PA. Calculations for stripping in the NIO1 can be found in [10]. The ratio between the total accelerated beam current I_{H^-} and I_{EG} may be taken as the e^-/H^- ratio. The current I_{EG} has been measured to be quite high (up to hundreds of mA) in these early operations and therefore it is generally limited via the LabVIEW interface of the power supply to 550-600 mA. This of course, together with discharge events between the grids, limits the possible combinations of pressure, RF power and extraction voltage and hence the achievable beam current. To increase the amount of negative ions, operation with O_2 instead of H_2 has also been performed due to the higher electronegativity of oxygen.

For continuous high power operations, a water cooled copper calorimeter is installed at the end of the beam-line, about 1.5 m downstream of the PG [5], with the double purpose of dumping the beam and diagnosing its main features. Up to now the accelerated current I_{H^-} has been quite low (few mA) and it was possible to operate the NIO1 for long pulses even with an uncooled calorimeter, as beam power with such a low current does not exceed 50 W. At present then, another calorimeter with a higher diagnostic capability has been installed to intercept the beam closer to the exit of the accelerator. This calorimeter consists of a 1D carbon-fibre-carbon composite (CFC) tile, as it will be the case for the SPIDER [4] calorimeter STRIKE [3]. In these early operations of the NIO1, only the CFC calorimeter has been used. The other beam diagnostic currently in operation is beam emission spectroscopy (BES).

The CFC tile adopted for NIO1 has a very large ratio between the thermal conductivity along the fibres and that in the planes normal to the fibres. This feature allows determination of the beam footprint by monitoring the temperature of the rear side of the tile (i.e. opposite to the beam) with an infra-red (IR) camera placed at the end of the vessel tube, as will be used for STRIKE. Tile dimensions are 125 × 91×12 mm^3. As the tile thickness is small and beam power is low, the temperature increase on the rear side does not differ much from that on the beam facing side. The tile is held between two C-shaped metallic supports, leaving space for thermal expansion at high temperatures. The base of the support lays directly on the bottom part of the vessel, as shown in Figure 2a. If the CFC tile is placed close enough to the PA so that it collects all the negative ions exiting the accelerator, the total H^- accelerated current can be determined as the sum of the current impinging on the PA and that impinging on the tile itself. In order to collect most of the ions on the tile, the distance d between the tile and the post-acceleration grid (PA) has been minimized as much as is achievable, allowing for other diagnostics, such as BES, to have some proper lines of sight

(LoS) to the beam. For most of the hereby reported measurements, the distance d was kept between 40 and 50 cm. The position of the tile with respect to the drift tube may be seen in Figure 2a.

When hydrogen gas is used, currents and voltages have been up to now quite limited because of the occurrence of discharge events in the accelerator. For this reason the power impinging on the tile is the order of a few Watts. The maximum signal strength obtained on the tile with H- beams is then quite poor (about 1 K/min as a peak). This of course is not practical for characterizing beam optics, as short pulses produce too small a ΔT, while longer pulses result in a temperature profile which is too broad. A larger signal strength, and hence an easier characterization, is obtained by using O^- beams. An estimate of the beam profile shape is given by its footprint on the tile, shown in Figure 2b, from which it may also be deduced that for pulses with bad optics, i.e. when beamlets have a divergence in the order of some degrees, some stray particles have hit the C-shaped supports. In the following sections both the direct and thermographic measurement of the current will be described. As this contribution focuses on the beam characterization by the CFC tile, most of the reported analysis will be based on O^- beams.

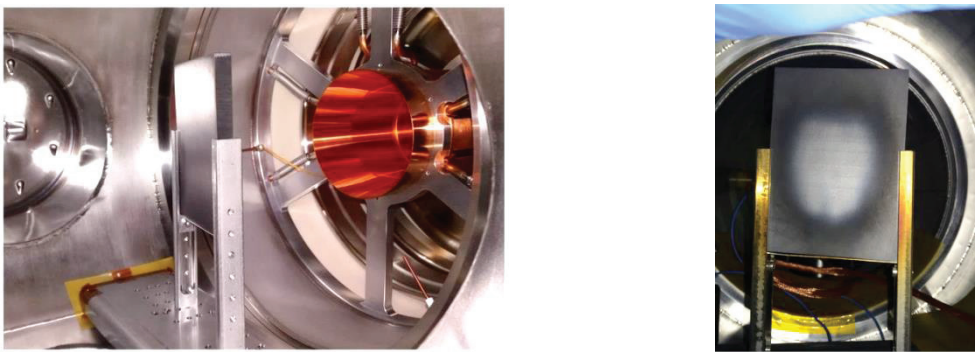

(a) (b)

Figure 2. (a) Position of the CFC tile inside the NIO1 vacuum vessel. (b) Beam facing side of the tile after few months of operation.

BEAM CURRENT MEASUREMENT

While the current hitting the grids of the accelerator system can be measured by the power supplies, the beam current impinging on the CFC tile is determined directly by measuring the voltage on a shunt resistor placed between the tile and ground. As already carried out at the NIFS test-stand [11], the tile has been biased to collect all the secondary electrons it emits when bombarded by the beam. During the test of this system, the measured beam current was quite low (about 10 μA) and R_s = 10 kΩ was used as a shunt to achieve a signal strength around 100 mV. It was found that a 50 V biasing was sufficient to saturate the signal from the tile (see Figure 3a), enhancing the measured value by about 20% with respect to the unbiased case. When currents reached the mA range, R_s was lowered to 0.333 kΩ.

Such measurements are affected by two possible sources of error. The first, which may lead to an under-estimation of the current, is that the fraction of H^- ions which have been converted to neutrals by stripping is not accounted for. On the other hand, tile biasing collects electrons from the plasma induced by the beam in the drift region, giving a possible over-estimation of the beam current. To reduce the collection of secondary electrons by the tile it is possible to bias the repeller. At present, the repeller is kept at the same potential of the tile (50 V).

As the IR camera provides a 2D map of the tile temperature increase $\Delta T(x,y)$, which is directly related to the impinging heat flux $Q(x,y)$, it allows a description of the variation of the beam dimensions (and hence of its divergence) due to changes in the source or accelerator parameters. At present, beam divergence is in general quite high and beamlets are not distinguishable in the IR image. This statement is confirmed by the current I_{PA} impinging on the post-acceleration grid, which has been up to now of the same order of magnitude of the current I_{CFC} measured at the tile. Simulations by the OPERA code suggest divergence should be greater than 20 mrad for the range of parameters used [12]. In such conditions, a first estimate of the quality of the beam optics may be given by the ratio I_{PA}/I_{CFC}.

Pressure, RF power, bias voltage, magnetic field, and extraction voltage are all variables which play a role in defining the beam current. Beam current, together with the extraction and acceleration voltage defines the beam optics. In particular, increasing the voltage ratio U_{tot}/U_{ex} may focus or de-focus the beam i.e. reduce or enlarge its divergence. The divergence is minimal for a certain optimal ratio which is expected to be higher for oxygen than for hydrogen due to its higher mass.

Keeping all other parameters fixed, it was verified that when changing U_{ex} or U_{tot}, the ratio I_{PA}/I_{CFC} also changes. In particular, the current ratio was found to have a minimum at a certain U_{tot}/U_{ex} and was found to increase either on increasing or reducing the voltage ratio from this point (see Figure 3b). Such a result suggests that the current ratio can be taken as a parameter to describe the beam optics when divergence is high enough so that a considerable part of the beam current impinges on the PA. As part of the beam current may hit the repeller, the current I_{REP} impinging on this grid has been measured and added to I_{PA} in the calculations. As shown in Figure 3, according to the current ratio, the best optics is found when U_{tot}/U_{ex} = 6-7 in hydrogen and when U_{tot}/U_{ex} = 9-10 in oxygen.

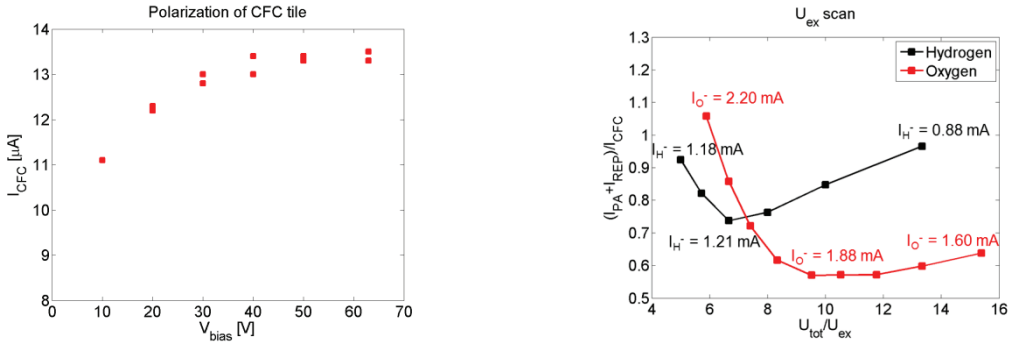

(a) (b)

Figure 3. (a) I-V characteristic for tile biasing. Oxygen beam, P_{RF} = 450 W, p_{source} = 0.18 Pa, U_{ex} = 1.2 kV, U_{tot} = 5 kV. (b) Current ratio $(I_{PA}+I_{REP})/I_{CFC}$ as a function of the voltage ratio. For H^-: P_{RF} = 1.1 kW, p_{source} = 0.28 Pa, U_{tot} = 8 kV, I_{filter} = 400 A. For O^-: P_{RF} = 800 W, p_{source} = 0.35 Pa, U_{tot} = 20 kV, I_{filter} = 400 A.

An estimate of the beam current may also be obtained also from the calorimetry of the tile. By fitting an exponential to the average temperature time trace both in the heating and the cooling phase, the beam power and hence its current can be calculated (see Figure 4a). The current from calorimetry I_{cal} is less affected by stripping, as power is also carried to the tile by neutrals, and it is not affected by secondary particles. This current estimate has been cross-checked with that from the electrical measurement. In the range 0.02-1.5 mA, the agreement between them was found to be quite successful. As shown in Figure 4b, a straight line can be fitted to the data, whose slope is comparable to unity.

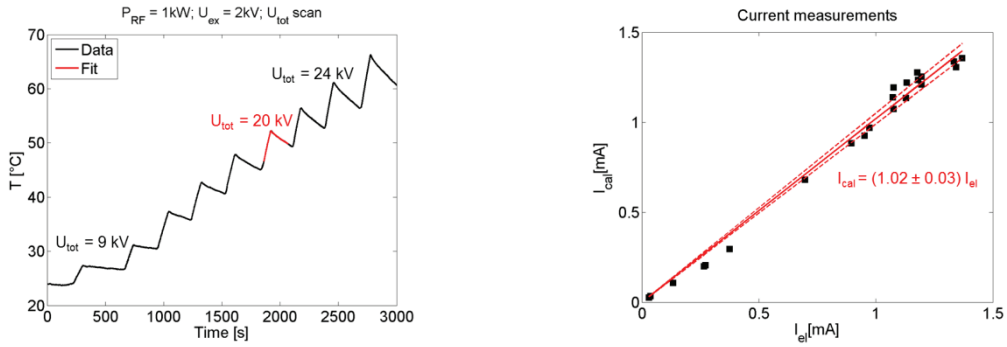

(a) (b)

Figure 4. (a) Time trace of the average tile temperature during one session of the NIO1 operation. (b) Correlation between calorimetric and electrical measurement of the beam current.

BEAM OPTICS ASSESSMENT BY THERMOGRAPHY

The distance between the IR camera and the CFC tile is large (about 1.8 m), limiting the spatial resolution of the measurement. The pixel-to-mm conversion is about 1.5 mm/pixel. Recently a new IR camera with a 0.9 mm/pixel resolution has been installed. To obtain a uniform emissivity, the tile surface has been polished. To avoid the disturbance due to the reflection of the camera lens itself onto a smooth surface, the tile has been tilted by 10° with respect to the plane normal to the beam. As cos(10°) = 0.984, the stretching along the horizontal direction of the heat flux impinging on the tile is negligible, while the distortion of the IR images due to the perspective is corrected in the data processing phase. The camera field of view is shown in Figure 5a. The sampling frequency has been fixed to 1-2 Hz as the increase of temperature is in most cases very slow, and with continuous operation there is a large amount of data. The beginning of the beam pulse is determined by looking at the temperature variation of a spot in the region hit by the beam. This estimate is of course not precise, as the heat takes time to propagate from the front to the rear side of the tile. At room temperature and for low power heat fluxes however, this delay is about 200-300 ms, which is less than the selected sampling time. Once the frame at which the beam starts is identified, the background temperature profile is subtracted to get ΔT(x,y), as shown in Figure 5b.

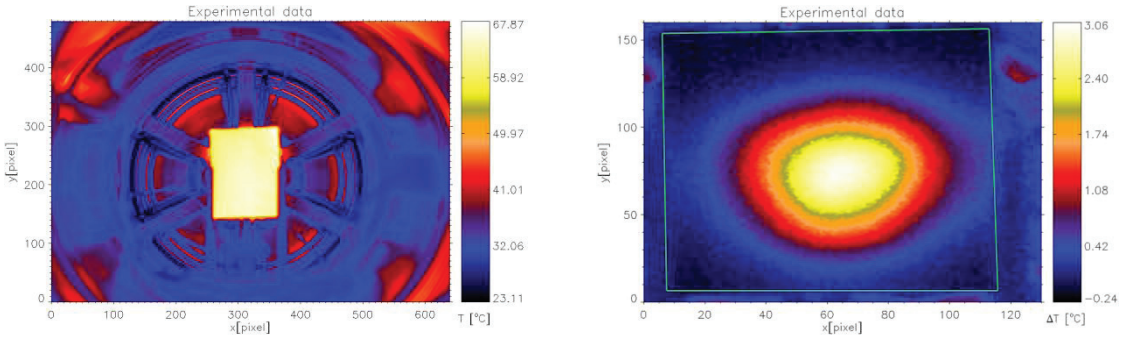

(a) (b)

Figure 5. (a) Camera field of view. (b) Map of the temperature increase of the tile rear surface. Tile borders are identified by the green line.

Due to the orientation of the permanent magnets in the EG, the deflection of the beam particles is in the vertical direction. In particular the right and left beamlet columns are deflected upward and the central one is deflected downward. The global beam shape is hence expected to be elongated in the vertical direction and its width in the horizontal direction is expected to be larger in the top than in the bottom part. The beam is hence expected to be trapezoidal when I_{PA}/I_{CFC} is low and more elliptical for worse optics, as shown in Figure 6. To compare different pulses a 1D temperature profile on a vertical line passing through the beam center can be taken. The comparison between two pulses with different current ratios is given in Figure 6.

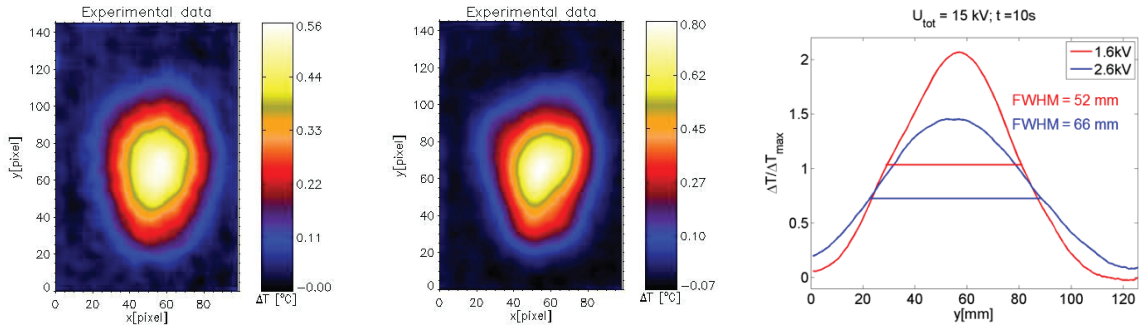

(a) (b) (c)

Figure 6. (a) ΔT map at t=3s for U_{tot} =15kV, U_{ex} =1.6kV, I_{PA}/I_{CFC} =0.2, oxygen. (b) ΔT map at t=3s for U_{tot} =15kV, U_{ex} = 2.6 kV, I_{PA}/I_{CFC} = 0.43, oxygen. (c) 1D temperature profile along a vertical line at t = 10s for pulses (a) and (b).

It can be seen that the full width at half maximum (FWHM) of the beam is smaller when the current ratio is lower, confirming the theory that I_{PA}/I_{CFC} can be taken as a parameter to describe beam optics. Figure 7a shows that the FWHM and the current ratio have a similar trend when plotted against the voltage ratio. The FWHM in the x direction is found to be about 30% smaller than that in the vertical direction. A possible explanation is that heat propagation is inhibited early by the tile borders more in the x direction than in the y direction, as the tile width is about 35% smaller than its height. This hypothesis is however not confirmed as a $FWHM_y/FWHM_x$ of approximately 1.3 is also found at the start of good optics pulses (see Figure 7b), when the 1D profile of ΔT, either vertical or horizontal, is very close to zero at the tile borders.

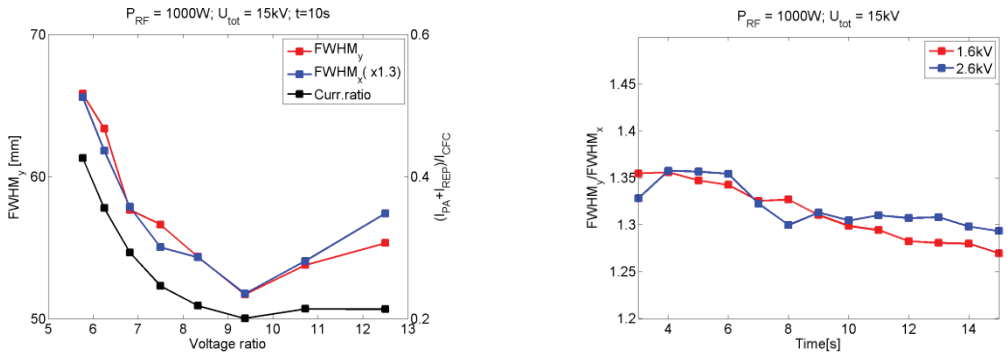

(a) (b)

Figure 7. (a) Dependence of the beam FWHM and current ratio on the voltage ratio U_{tot}/U_{ex}. (b) Ratio of the beam vertical and horizontal width as a function of time. Accelerator and source parameters are the same as in Figure 6.

Another effect to be taken into account is that of Coulomb repulsion among beamlets, which can be quite large depending on the distance over which the beamlets are space charge compensated. By modeling a beamlet as a current carrying wire, the deflection of a particle belonging to a neighbor beamlet may be estimated as a function of the length required for a full space charge compensation to occur. Deflection may be up to tens of mrad. As the electrostatic repulsion has no preferential direction, it tends to reduce the beam ellipticity. To explain what is found experimentally, the Coulomb repulsion should be considered to be almost negligible meaning that a short distance is required for space charge compensation to occur.

An attempt to reproduce the beam shape can be done by neglecting the Coulomb repulsion and considering a rigid displacement of the beamlet columns to describe the magnetic deflection. The heat flux of each beamlet is modeled as a 2D Gaussian with a standard deviation given by $\sigma = \sigma_0 + d \cdot \alpha$, where α is the beamlet divergence and σ_0 the standard deviation at the exit of the PA. Fixing the beam power to that calculated from the current and voltage measurement, the magnetic deflection and the beam divergence have been changed so as to generate heat loads with same integral but different shapes. The simulated heat loads have been taken as input in a COMSOL finite element model to determine what would be the temperature map seen by the camera for each divergence-deflection combination. The results of this analysis for case (a) of Figure 6 are reported in Figure 8. In this case it was found that in order to explain the shape of the beam, a large magnetic deflection (about 35 mrad) and a relatively small divergence (1°) would be necessary.

With these assumptions, the maximum temperature found in the simulation was consistent with the experimental measurement by assuming an underestimation of about 15% in the current measurement. Unfortunately similar estimates are not in agreement with beam simulations (by the OPERA code) in the same conditions. OPERA in fact produces a more divergent and less deflected (i.e. more circular) beam. In particular for the same current and voltages, an 11 mrad deflection and a 2° divergence were found [12]. Further investigations are hence necessary and will be carried out in the future to explain this discrepancy. A possible explanation of a larger than expected magnetic deflection could be to assume an asymmetric meniscus [11]. Another hypotheses which could explain a very elongated beam shape is a reduced intensity of one of the outer beamlet columns[14].

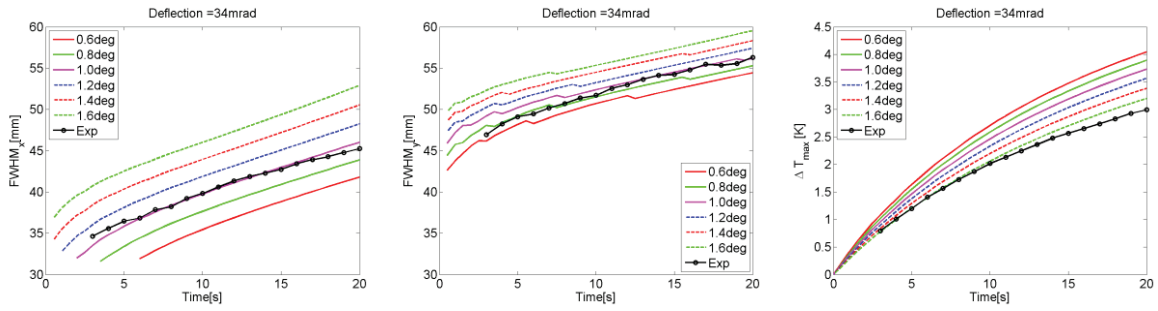

Figure 8. Comparison between experimental data and simulation output for a 34 mrad upward/downward magnetic deflection and different beamlet divergences. (a) $FWHM_x$, (b) $FWHM_y$, (c) Maximum temperature.

The importance of the beam deflection may be verified by considering pulses in hydrogen. As it can be seen in Figure 9, the beam width in the vertical direction may change greatly by changing the extraction voltage. By doubling U_{ex}, the $FWHM_y$ is reduced by a 30% (from 81 mm to 56 mm) and the general trend of $FWHM_y$ is decreasing for increasing U_{ex}. On the other hand, for the trend of $FWHM_x$ w.r.t to U_{tot}/U_{ex}, a minimum can be identified around $U_{tot}/U_{ex} = 8$, not dissimilar from the minimum of the ratio I_{PA}/I_{CFC}. A similar stretching of the beam for low extraction voltages is consistent with the expected $U_{ex}^{-1/2}$ deflection due to the magnetic field. For hydrogen therefore, the observed global beam shape is mainly due to beam deflection by the magnetic field, while in the case of oxygen the deflection is smaller and the effect of divergence variation can be seen. In particular for the O^- beam, a minimum is found for the FWHM in both directions as a function of the voltage ratio, and this minimum is the same for both $FWHM_x$ and $FWHM_y$. This difference between the two species could be simply explained by the use of larger U_{ex} (from 1.2 kV to 2.6 kV) and by the higher mass of oxygen.

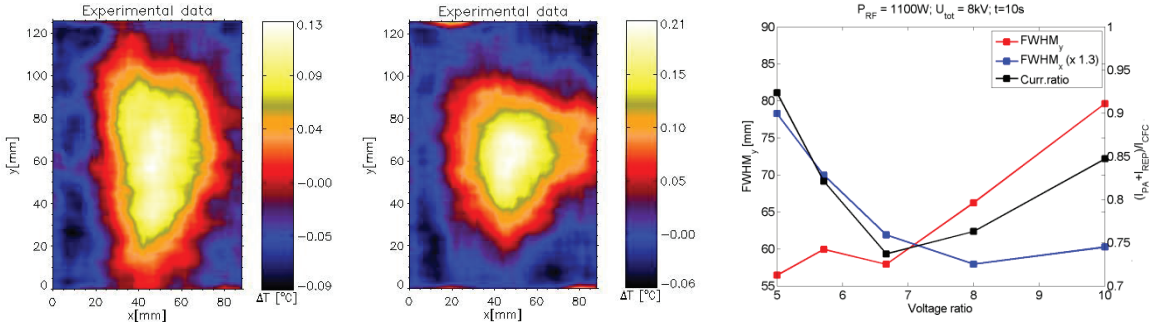

Figure 9. (a) ΔT map at t = 10s for U_{tot} = 8kV, U_{ex} = 0.8kV, I_{PA}/I_{CFC} = 0.85, hydrogen. (b) ΔT map at t=10s for U_{tot} = 8kV, U_{ex} = 1.6 kV, I_{PA}/I_{CFC} = 0.92, hydrogen. (c) Dependence of the beam FWHM and of the current ratio on the voltage ratio U_{tot}/U_{ex}.

CONCLUSION

A 1D-CFC tile is currently being exposed to the NIO1 ion beam and used as a diagnostic calorimeter. Its rear surface is observed by a thermal camera to characterize the beam in terms of total current and profile shape. A direct electrical measurement of the current impinging on the tile has also been possible by measuring the voltage over a shunt resistor placed in series with the tile. This measure of the beam current has been successfully cross-checked with the estimate from the CFC tile calorimetry. The large ratios (in the range 0.2-1.5) between the current impinging on the post-acceleration grid and that hitting the CFC tile suggests that beamlet divergence is quite high, as expected for low current operation. Beamlets are in fact not yet distinguishable even if a global trapezoidal shape can be identified. This is due to the alternate deflection of the beamlet columns in the vertical direction caused by the alternate orientation of the permanent magnets in the EG. The maximum beam current achieved at present has been about 2 mA in

hydrogen and 3 mA in oxygen, the latter which has been largely used in the tests on the extraction system due to its higher electronegativity. The beam divergence in this beam current range, is in general larger than 1°. Variations of the beam FWHM can be seen on the calorimeter as voltages are changed. In the case of oxygen, the minimum width is found for the same voltage ratio which minimizes the ratio between the current I_{PA} impinging onto the post-acceleration grid and that impinging on the tile I_{CFC}. In the case of hydrogen, it was possible to find the best voltage ratio only for the beam width in the horizontal direction, which is not affected by the magnetic deflection. For the vertical direction, the beam FWHM was simply found to increase by decreasing the extraction voltage. This behavior suggests that the beamlet deflection is large enough in this range of U_{ex} to overcome the effects of the optics. As deflection is proportional to $U_{ex}^{-1/2}$, the effect of variation of the voltage ratio is expected to be seen clearly when the extraction voltage is increased. The best optics condition was found to be when the ratio I_{PA}/I_{CFC} was around 6-7 for hydrogen and 9-10 for oxygen. Better performances could be achieved with different filter field configurations [8] and with a new design of the extraction grid [13]. In such conditions an easier and more detailed characterization of the NIO1 beam is also expected.

The CFC tile presently used may be substituted in the few next months by a larger tile. Consorzio RFX has in fact recently tested the new prototypes for the STRIKE tiles. As well as the full size prototype, two half size samples (188 × 142 × 20 mm^3) have also been provided by the manufacturer and have shown thermal properties similar to those of the present solution [15]. If these samples are successful in tests on their resistance to thermo-mechanical stress [16], one of them could be installed inside the NIO1 vacuum vessel. This would ensure collection of all of the beam current, even for pulses with very large divergence. The use of these prototype tiles would reduce the temperature resolution (due to the larger thickness of the tile); on the other hand their higher thermal capacity would increase the duty cycle of the operations.

ACKNOWLEDGMENTS

This work was set up with partial financial support of EUROfusion.

REFERENCES

1. M.Cavenago et al. AIP Conf. Proc. **1515**, 157 (2013).
2. B.Zaniol et al. AIP Conf. Proc. **1655**, 060010 (2015).
3. A. Rizzolo et al. Fusion Eng. Des. **85**, 2268 (2010).
4. P.Sonato et al. Fusion Eng. Des. **84**, 269 (2009).
5. M. Cavenago et al. Rev.Sci.Instrum. **85** 02A704 (2014).
6. M. Cavenago et al. Rev.Sci.Instrum. **87** 02B320 (2016).
7. M. Cavenago et al. *Improvements of the Versatile Multiaperture Negative Ion Source NIO1*, these proceedings.
8. P.Veltri et al. *Study of electron transport across the magnetic filter of NIO1 Negative ion Source*, these proceedings.
9. E. Speth et al. Nucl.Fusion **46**, S220 (2006).
10. E. Sartori et al. Rev.Sci.Instrum. **87** 02B118 (2016).
11. P. Veltri et al. *Ion beam transport: modeling and experimental measurements on a large negative ion source in view of the ITER heating neutral beam*, submitted to Nuclear Fusion.
12. C.Baltador, private communication.
13. C.Baltador et al., *Finite elements numerical codes as primary tool to improve beam optics and support measurements in NIO1*, these proceedings.
14. G.Chitarin et al. *Experimental validation of an innovative deflection compensation method in a multi-beamlet negative-ion accelerator*, these proceedings.
15. G. Serianni et al. *Test of 1D carbon-carbon composite prototype tiles for the SPIDER diagnostic calorimeter*, these proceedings.
16. M. De Muri et al. Rev.Sci.Instrum. **85** 02A718 (2014).